journal

Reprinted from the Journal of the American Ceramic Society, Vol. 74, No. 4, April 1991

J. Am. Ceram. Soc., 74 [4] 767–71 (1991)

Kinking of a Crack out of an Interface: Role of In-Plane Stress

Ming-Yuan He, Andrew Bartlett,* and Anthony G. Evans*

Materials Department, College of Engineering, University of California, Santa Barbara, California 93106

John W. Hutchinson*

Division of Applied Sciences, Harvard University, Cambridge, Massachusetts 02138

A crack lying in the interface between two brittle elastic solids can advance either by continued growth in the interface or by kinking out of the interface into one of the adjoining materials. This competition can be assessed by comparing the ratio of the energy release rates for interface cracking and for kinking out of the interface to the ratio of interface toughness to substrate toughness. The stress parallel to the interface, σ_0, influences the energy release rate of the kinked crack and can significantly alter the conditions for interface cracking over substrate cracking if sufficiently large. This paper provides the dependence of the energy release rate ratio on the in-plane stress. The nondimensional stress parameter which emerges is, $\sigma_0(a/E_* \Gamma_i)^{1/2}$, where a is the initial length of the kink into the substrate, E_* is a modulus quantity, and Γ_i is the fracture energy of the interface. An experimental observation of the cracking of reaction product layers in bonds between Ti(Ta) and Al_2O_3 is rationalized by the theory. [Key words: crack growth, interfaces, kinking, stress, fibers.]

I. Introduction

In an earlier paper (He and Hutchinson,[1] hereafter designated by HH), a study was made of the tendency of a crack in an interface to either remain in the interface or kink out (Fig. 1). The ratio $\mathcal{G}_i/\mathcal{G}_s^{max}$ was determined where $\mathcal{G}_i$ is the energy release rate for crack advance in the interface and $\mathcal{G}_s^{max}$ is the energy release rate for the crack kinking into the substrate maximized with respect to the kink angle ω. The competition between interface cracking and substrate cracking then depends on whether $\mathcal{G}_i/\mathcal{G}_s^{max}$ is greater or less than the toughness ratio, Γ_i/Γ_s, where Γ_i and Γ_s are the interface and substrate toughnesses, respectively.

The analysis in HH is an asymptotic one in which the prediction of $\mathcal{G}_i/\mathcal{G}_s^{max}$ is accurate when the length a of the kinked crack segment is very small compared to all other lengths in the problem, including the length of the parent interface crack itself. If there is a stress σ_0 in the substrate parallel to the interface (Fig. 1) due to either residual stress or applied loads, then an additional nondimensional length parameter, not considered in HH, becomes important:

$$\eta = \sigma_0 \sqrt{a}/(E_* \mathcal{G}_i)^{1/2} \tag{1}$$

where E_* is a modulus quantity defined below. The role of this parameter in the competition between kinking and continued interface cracking is the subject of this paper. An experimental observation of the cracking at the reaction product layer formed upon bonding Ti(Ta) to Al_2O_3 is used to illustrate the phenomenon.

II. Stress Intensity Factors and Energy Release Rates for a Kinked Crack

As in HH, it will be assumed that the putative length a of the kinked crack is very small compared with all other geometric length quantities and, in particular, small compared with the length of the parent interface crack. Under these circumstances, an asymptotic problem can be posed, as depicted in Fig. 1(B). Notably, a semi-infinite interface crack is loaded remotely by the singular crack tip field associated with the interface crack of Fig. 1(A), with stress intensity factors K_1 and K_2 and by the stress σ_0 parallel to the interface located in the material into which the crack kinks.† In an application, the stress intensity factors K_1 and K_2 are regarded as the applied stress intensities and are determined for the interface crack in the actual geometry.

Plane strain cracks are considered, and the two materials bonded at the interface (Fig. 1) are assumed to be isotropic and elastic. The two elastic mismatch parameters of Dundurs governing plane strain problems are

$$\alpha = (\bar{E}_1 - \bar{E}_2)/(\bar{E}_1 + \bar{E}_2) \tag{2}$$

$$\beta = \frac{1}{2}[\mu_1(1 - 2\nu_2) - \mu_2(1 - 2\nu_1)]/[\mu_1(1 - \nu_2) + \mu_2(1 - \nu_1)] \tag{3}$$

†Only the stress component in the material into which the kink extends has any effect on the change in energy release rate.

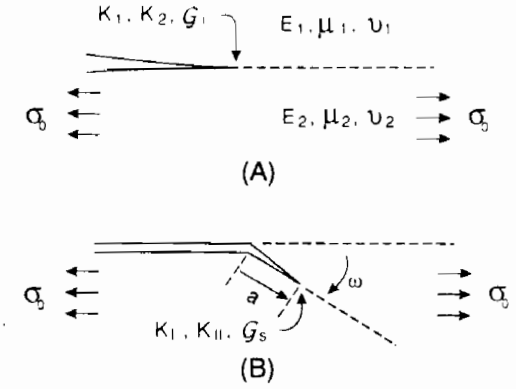

Fig. 1. Notation and conventions: (A) interface crack, (B) kinked crack.

R. F. Cook—contributing editor

Manuscript No. 197664. Received April 4, 1990; approved December 12, 1990.
*Member, American Ceramic Society.

where E, μ, and ν denote Young's modulus, shear modulus, and Poisson's ratio, respectively, and $\bar{E} = E/(1 - \nu^2)$. The condition $\alpha = \beta = 0$ refers to a homogeneous system. An "oscillation index" ε, which appears below, depends only on β according to

$$\varepsilon = \frac{1}{2\pi} \ln\left(\frac{1-\beta}{1+\beta}\right) \tag{4}$$

A general discussion of elastic interface cracks has been given by Rice.[2] For a specific problem, the complex interface stress intensity factor necessarily has the dimensional form (with $i = (-1)^{1/2}$)

$$K \equiv K_1 + iK_2 = (\text{applied stress}) \cdot L^{1/2} L^{-i\varepsilon} F \tag{5}$$

where L is a length (e.g., the parent crack length or layer thickness) and F is a dimensionless function of parameters characterizing the in-plane geometry and of α and β. The tractions on the interface ahead of the interface crack tip (still with $a = 0$) are given by

$$\sigma_{22} + i\sigma_{12} = K(2\pi x_1)^{-1/2} x_1^{i\varepsilon} \tag{6}$$

When $\beta = 0$, and thus $\varepsilon = 0$ so that $x_1^{i\varepsilon} = 1$, K_1 and K_2 can be regarded as conventional mode 1 and mode 2 stress intensity factors, i.e.,

$$\sigma_{22} = K_1(2\pi x)^{-1/2}$$
$$\sigma_{12} = K_2(2\pi x_1)^{-1/2} \tag{7}$$

As emphasized in Ref. 3, the clarity in interpretation achieved by taking β to be zero is often worth the small sacrifice in accuracy.

It will be useful for later purposes to introduce the "phase" ψ of the stress intensity factors. With L defined in Eq. (5),

$$K \equiv K_1 + iK_2 = |K| e^{i\psi} L^{-i\varepsilon} \tag{8a}$$

or

$$\tan\psi = I_m[KL^{i\varepsilon}]/R_e[KL^{i\varepsilon}] \tag{8b}$$

In particular, when $\beta = 0$

$$\psi = \tan^{-1}(K_2/K_1) \tag{9}$$

and ψ provides a measure of the relative amount of mode 2 to mode 1 of the loading on the interface crack.

The energy release rate for advance of the crack in the interface is

$$\mathcal{G}_i = (K_1^2 + K_2^2)/E_* \tag{10}$$

where

$$\frac{1}{E_*} = \frac{1}{2}\left[\frac{1}{\bar{E}_1} + \frac{1}{\bar{E}_2}\right] \frac{1}{\cosh^2 \pi\varepsilon} = \left(\frac{1-\beta^2}{1+\alpha}\right)\frac{1}{\bar{E}_2} \tag{11}$$

The stress component σ_0 has no effect on $\mathcal{G}_i$, since it acts parallel to the advancing crack.

The tip of the putative crack kinking into the substrate in Fig. 1(B) experiences conventional mode I/mode II stressing characterized by stress intensity factors K_I and K_{II}. The relationship between the intensity factors of the kinked crack and those of the parent interface crack is expressed compactly as

$$K_I + iK_{II} = cKa^{i\varepsilon} + \bar{d}\bar{K}a^{-i\varepsilon} + b\sigma_0 a^{1/2} \tag{12}$$

where $(\bar{\ })$ denotes the complex conjugate. Here c, d, and b are dimensionless complex functions of ω, α, and β. The argument leading to the K terms in Eq. (12) is based primarily on simple dimensional considerations given in HH. The σ_0 term can be justified solely on the grounds that K_I and K_{II} depend linearly on σ_0 and that the only length quantity in the elasticity problem is a.

The calculations of $b \equiv b_1 + ib_2$ use the integral equation formulation of HH. The present results were obtained using the previous numerical scheme simply by changing the "loading on the crack" to be that associated with σ_0. Curves of b_1 and b_2 as functions of ω for various α, all with $\beta = 0$, are shown in Fig. 2. There is virtually no dependence of b_1 and b_2 on β. For example, the values computed with $\beta = \alpha/4$ differ from those computed with $\beta = 0$ by no more than about 1%. (The connection $\beta = \alpha/4$ corresponds with $\nu_1 = \nu_2 = 1/3$, typical for many material combinations.)[4] An approximate solution for the case of no elastic mismatch is readily obtained from the formulas given in Ref. 5. That approximation is

$$b_1 = 2(2/\pi)^{1/2} \sin^2\omega$$
$$b_2 = (2/\pi)^{1/2} \sin 2\omega \tag{13}$$

and, as shown by the dashed curve in Fig. 2, gives a good approximation for $\alpha = \beta = 0$ when ω is less than about 60°.

The real and imaginary parts of $c = c_R + ic_I$ and $d = d_R + id_I$ have been tabulated as functions of ω for a wide range of combinations of α and β.[6] When $\beta = 0$, Eq. (12) can be written as

$$K_I = (c_R + d_R)K_1 - (c_I + d_I)K_2 + b_1\sigma_0 a^{1/2} \tag{14}$$

$$K_{II} = (c_I - d_I)K_1 + (c_R - d_R)K_2 + b_2\sigma_0 a^{1/2} \tag{15}$$

The energy release rate of the kinked crack is

$$\mathcal{G}_s = (K_I^2 + K_{II}^2)/\bar{E}_2 \tag{16}$$

such that, with Eq. (12)

$$\mathcal{G}_s = (\mathcal{G}_s)_{\eta=0} + 2\sigma_0 a^{1/2} R_e[\bar{b}(cKa^{i\varepsilon} + \bar{d}\bar{K}a^{-i\varepsilon})]/\bar{E}_2 + (b_1^2 + b_2^2)\sigma_0^2 a/\bar{E}_2 \tag{17}$$

where

$$(\mathcal{G}_s)_{\eta=0} = \{(|c|^2 + |d|^2)K\bar{K} + 2R_e(cdK^2 a^{2i\varepsilon})\}/\bar{E}_2 \tag{18}$$

This last quantity is the energy release rate when $\sigma_0 = 0$. The ratio of the two release rates is obtained from Eqs. (10) and (17) using Eq. (8) as

$$\mathcal{G}_s/\mathcal{G}_i = f^{(0)}(\omega_1, \tilde{\psi}) + \eta f^{(1)}(\omega_1\tilde{\psi}) + \eta^2 f^{(2)}(\omega) \tag{19}$$

where η is defined in Eq. (1) and

$$f^{(0)} = ((1+\alpha)/(1-\beta^2))\{|c|^2 + |d|^2 + 2R_e[cde^{2i\tilde{\psi}}]\}$$
$$f^{(1)} = 2((1+\alpha)/(1-\beta^2))R_e\{\bar{b}[ce^{i\tilde{\psi}} + \bar{d}e^{-i\tilde{\psi}}]\}$$
$$f^{(2)} = ((1+\alpha)/(1-\beta^2))(b_1^2 + b_2^2)$$

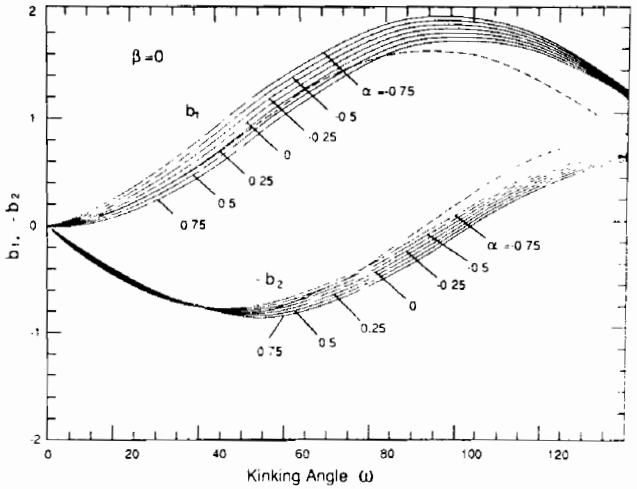

Fig. 2. Curves of b_1 and b_2 as a function of ω for various α. The dashed line curve is the approximation (13).

with

$$\tilde{\psi} = \psi + \varepsilon \ln (a/L)$$

The functions $f^{(i)}$ are independent of the magnitude of K but depend on the phase ψ of the interface stress intensity factors, as well as on the kink angle ω. If $\beta = 0$, these functions are independent of the putative crack length a, and therefore $\mathcal{G}_s/\mathcal{G}_i$ depends on a only through η. When $\beta \neq 0$, there is an additional *very weak* dependence on a through term $\varepsilon \ln (a/L)$ in $f^{(0)}$ and $f^{(1)}$. In what follows, the focus is on material mismatches with $\beta = 0$, either exactly or approximately. This choice averts the (usually nonessential) complications associated with the weak $\varepsilon \ln (a/L)$ dependence. Some assessment of the effect of nonzero β values can be obtained from the results presented below by simply accounting for the contribution $\varepsilon \ln (a/L)$ to $\tilde{\psi}$. This term amounts to a phase shift in ψ. Some further discussion of how this dependence affects the behavior when σ_0 vanishes is given in HH.

III. Interface Cracking versus Kinking

The role played by σ_0 on the competition between continued interface cracking and kinking into the substrate is illustrated in Figs. 3 and 4. The ratio $\mathcal{G}_i/\mathcal{G}_s$, as calculated from Eq. (19), is plotted in Fig. 3 as a function of the kink angle ω for the case $\alpha = \beta = 0$. The parent interface crack is loaded with equal amounts of mode 1 and mode 2 ($\psi = 45°$). The stress σ_0 begins to have an appreciable effect on the release rate ratio when $|\eta|$ is about 1/10; furthermore, when $|\eta|$ is 1/4, the $\mathcal{G}$ ratio is increased or decreased by about 50%, depending on the sign of σ_0.

The ratio $\mathcal{G}_i/\mathcal{G}_s^{max}$ is plotted as a function of ψ in Fig. 4, again for the case $\alpha = \beta = 0$. Here, $\mathcal{G}_s^{max}$ is the value of $\mathcal{G}_s$ maximized with respect to the kink angle ω. As detailed in HH for the limit $\eta = 0$, the value of ω at which $\mathcal{G}_s$ is maximized usually corresponds very closely (but not exactly) to the direction of the kink corresponding to $K_{II} = 0$. A significant difference between these two directions occurs only when the material into which the crack kinks is substantially stiffer than the other material, and then only when the loading on the interface crack is heavily mode 2.

Consider the role of *in-plane tension* ($\eta > 0$) with the aid of Fig. 4. Determine $\mathcal{G}_i/\mathcal{G}_s^{max}$, given the mode of loading as specified by ψ and the value of η based on estimates of initial flaw size a and σ_0. Let $\Gamma_i(\psi)$ be the mode-dependent interface toughness and $\Gamma_s = K_{IC}^2/\bar{E}_2$, the mode I toughness of the substrate material. If

$$\Gamma_i/\Gamma_s < \mathcal{G}_i/\mathcal{G}_s^{max} \tag{20}$$

the interface crack meets the condition for continuing advance in the interface at an applied load too low to advance the flaw into the substrate. Conversely, if the inequality in Eq. (20) is reversed, the flaw initiates a kink at an applied load lower than that necessary to advance the crack in the interface. The *transition toughness ratio* separating interface cracking from substrate kinking is given by

$$(\Gamma_i/\Gamma_s)_{TRANSITION} = \mathcal{G}_i/\mathcal{G}_S^{max} \tag{21}$$

The curves in Fig. 4 thus provide the transition toughness ratio for a given mode of loading and a given η. Note that at the transition, $\mathcal{G}_i$ can be replaced by Γ_i in the expression (1) for η. For this case, once substrate cracking is initiated, η increases as the crack grows, further increasing the driving force on the tip of the crack, and the kink becomes unstable.

In-plane compression in the substrate ($\eta < 0$) leads to very different behavior. In this case, $\mathcal{G}_s$ decreases with increasing a, and cracks which kink into the substrate tend to arrest. To further examine this phenomenon, let

$$\Delta = \Gamma_i/\Gamma_s - (\mathcal{G}_i/\mathcal{G}_S^{max})_{\eta=0} \tag{22}$$

If $\Delta < 0$, interface cracking occurs and substrate cracks will not be initiated. If $\Delta > 0$, sufficiently small flaws will initiate kink cracks but, because η decreases (as a increases), these will subsequently arrest when

$$\mathcal{G}_S^{max} = \Gamma_s \tag{23}$$

Now imagine a three-dimensional interface crack front encountering small flaws in the substrate. When σ_0 is compressive and $\Delta > 0$, *it is possible to have interface cracking* (with $\mathcal{G}_i = \Gamma_i$) *and still initiate small cracks which kink into the substrate and then arrest upon growth to a length governed by Eq. (23).*

The effect of elastic mismatch on $\mathcal{G}_i/\mathcal{G}_s^{max}$ is shown in Figs. 5 and 6 for ($\alpha = 0.5$, $\beta = 0$) and ($\alpha = -0.5$, $\beta = 0$), respectively. All other things being equal, increasing the relative compliance of the material into which the crack kinks increases the energy release rate of the kinked crack, and thus increases the tendency for substrate cracking.

To facilitate estimation of the effects of in-plane stress, the lowest order influence of η on the release rate ratio is expressed as

$$\mathcal{G}_i/\mathcal{G}_S^{max} \cong (\mathcal{G}_i/\mathcal{G}_S^{max})_{\eta=0} - \eta f(\alpha, \psi) \tag{24}$$

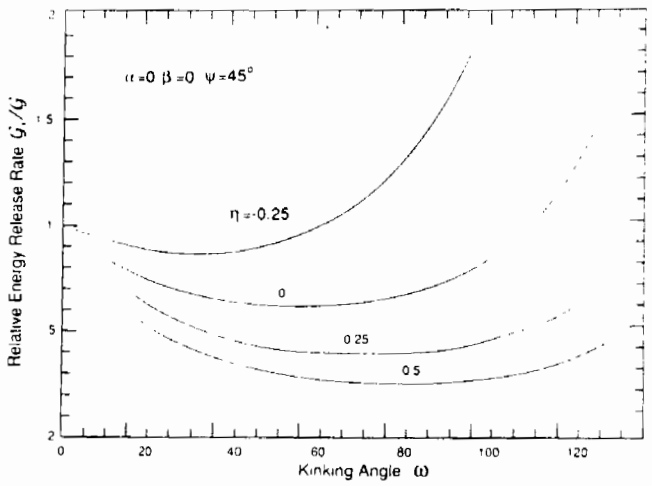

Fig. 3. Energy release rate ratio as a function of the kinking angle ω for various values of the residual stress parameter η; $\psi \equiv \tan^{-1}(K_2/K_1) = 45°$ and $\alpha = \beta = 0$.

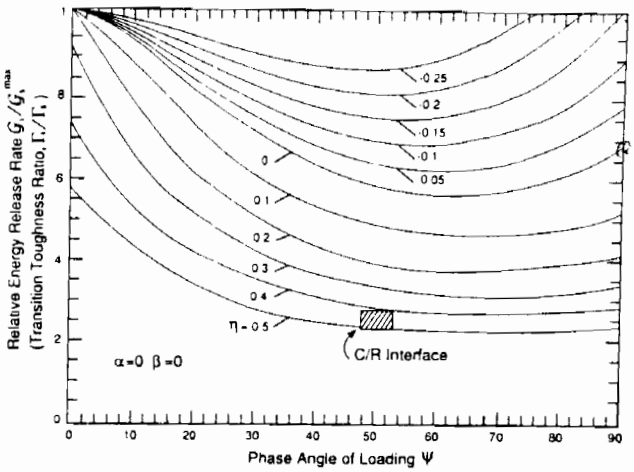

Fig. 4. Ratio of interface energy release rate to maximum energy release rate of kinked crack as a function of the phase of loading $\psi \equiv \tan^{-1}(K_2/K_1)$ for various values of the in-plane stress parameter η. $\alpha = \beta = 0$. The interpretation as the transition toughness ratio, Γ_i/Γ_s, applies only for $\eta > 0$. The datum is discussed in Section IV.

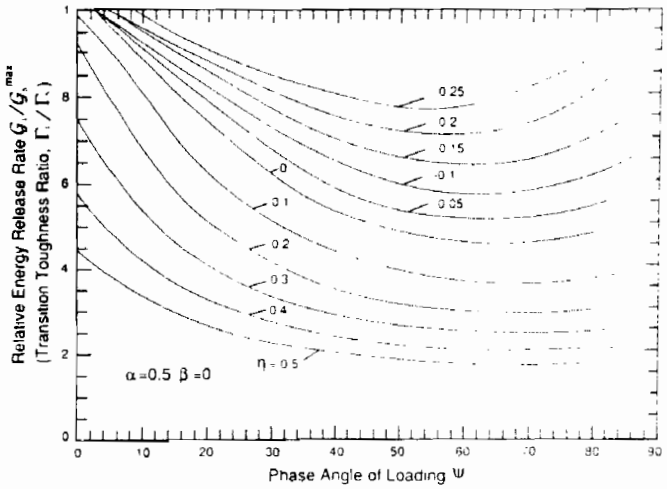

Fig. 5. Energy release rate ratio versus ψ for $\alpha = 0.5$, $\beta = 0$

This result is obtained from Eq. (19) with

$$(\mathcal{G}_i/\mathcal{G}_s^{max})_{\eta=0} = 1/f^{(0)}(\omega^*,\psi)$$

$$f = f^{(1)}(\omega^*,\psi)/f^{(0)}(\omega^*,\psi)^2 \tag{25}$$

where ω^* is the value of ω which maximizes $f^{(0)}(\omega,\psi)$. Curves of $(\mathcal{G}_i/\mathcal{G}_s^{max})_{\eta=0}$ and f as functions of ψ for various α (with $\beta = 0$) are shown in Figs. 7(A) and (B). Comparison of Eq. (24) with the full numerical results in Figs. 4 to 6 reveals that the approximation retains accuracy to within about 10% for $|\eta| \lesssim 0.2$.

Based on this approximation, the transition toughness ratio shifts with tensile in-plane stress according to

$$(\Gamma_i/\Gamma_s)_{TRANSITION} \cong (\mathcal{G}_i/\mathcal{G}_s^{max})_{\eta=0} - \eta f(\alpha,\psi) \tag{26}$$

When σ_0 is compressive, the length of the arrested kink cracks can also be estimated using Eq. (24) when $|\eta| \lesssim 0.2$. Suppose, as discussed earlier, that Δ in Eq. (22) is positive. Using Eq. (24) with the arrest condition (Eq. (23)) gives

$$-\eta = (-\sigma_0)(a/(E_*\Gamma_i))^{1/2} \cong \Delta/f \tag{27}$$

IV. Experimental Illustration

An experimental illustration of the importance of the above calculations concerns cracking in a diffusion bonded system between Ti(Ta) and Al_2O_3. Upon diffusion bonding, brittle reaction products form in this system, consisting of various intermetallics,[7,8] including the γ, α_2, and σ phases in the Ti, Al, Ta ternary. These layers are typically 3 μm thick

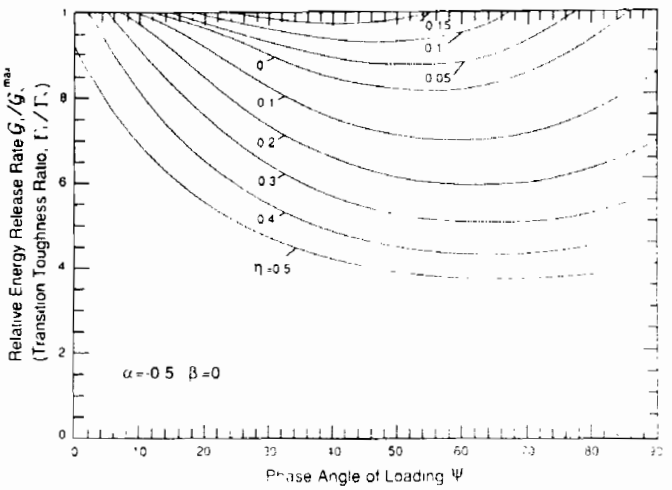

Fig. 6. Energy release rate ratio versus ψ for $\alpha = -0.5$, $\beta = 0$

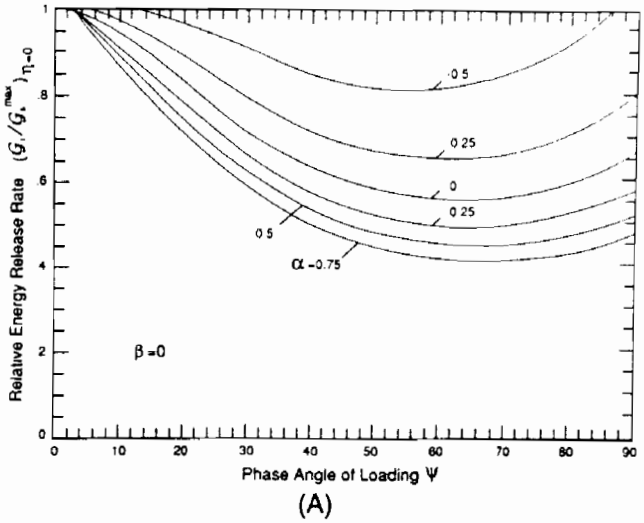

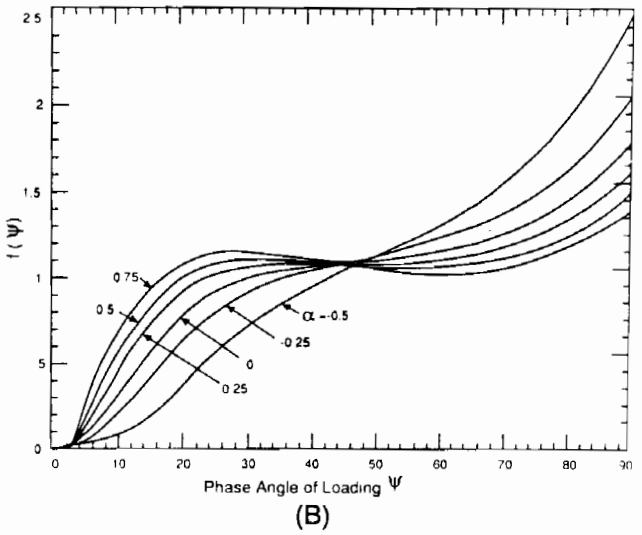

Fig. 7. (A) Energy release rate ratio versus $\psi \equiv \tan^{-1}(K_2/K_1)$ for $\eta = 0$. (B) Coefficient of lowest order contribution of η to energy release rate ratio in Eq. (24). In both cases, $\beta = 0$.

(Fig. 8). Interface fracture energy measurements have been made on this system using a notched flexural specimen.[7] Two observations and measurements are relevant. When precracking is conducted in three-point flexure, the crack introduced into the Al_2O_3, which extends normal to the interface, penetrates the reaction product layer and arrests at the reaction product/Ti interface (Fig. 8(A)), referred to as the R/M interface. Subsequent to precracking, when the specimen is loaded in four-point bending, cracks nucleate at the Al_2O_3/reaction product interface, referred to as the C/R interface, and propagate along that interface (Fig. 8(B)). The associated propagation load[7] indicates a fracture energy for this interface of $\Gamma_i \approx 17\ J \cdot m^{-2}$. Also, periodic branch cracks are emitted into the reaction product layer as the primary crack extends along the interface. These branch cracks arrest at the R/M interface (Fig. 8(B)). Cross sections suggest that the branch cracks tunnel across the reaction product layer, starting from the free edge. It is apparent from these results that the R/M interface has a relatively high fracture energy and is not a factor in the fracture process. Independent measurements of the fracture energy of reaction products in Ti/Al, refractory metal ternary systems, such as the σ phase,[9] indicate values in the range $\Gamma_R \approx 40$ to $50\ J \cdot m^{-2}$. This multiplicity of fracture behaviors can be rationalized using the preceding calculations.

During precracking, with the mode I crack in the Al_2O_3 normal to the interface, the fracture energy ratio between the

(A)

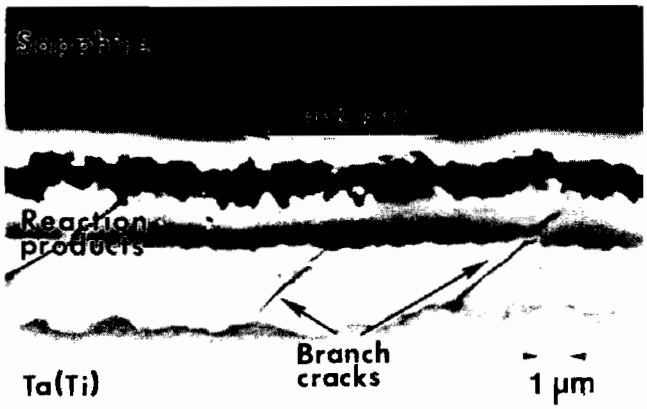

(B)

Fig. 8. (A) A precrack that extended in the Al_2O_3 normal to the interface and propagated through the reaction product interface in a Ti(Ta)/Al_2O_3 bond. (B) A mixed-mode crack extending along the Al_2O_3/reaction product layer interface. Also shown are periodic, inclined branch cracks in the reaction product layers formed upon interface crack extension.

reaction products and the C/M interface is $\Gamma_i/\Gamma_R \approx 1/3$. This ratio is in a range consistent with the observed crack penetration into the reaction products.[10] Upon subsequent loading, when crack extension occurs along the C/R interface, the phase angle ψ is approximately 50°.[11] For this case, with $\eta = 0$ and $\Gamma_i/\Gamma_R \approx 1/3$, Fig. 4 would indicate that the crack *should remain at the C/R interface.* However, if a tensile misfit stress exists within the reaction product layer, Fig. 4 indicates that $\eta \approx 0.5$ *would allow the formation of branch cracks.* Based on the elastic properties of the Ti/Al_2O_3 system,[7] the requirement for branch cracking becomes, $\sigma_0(c)^{1/2} \approx 1\ \text{MPa} \cdot \text{m}^{1/2}$. Since the branch cracks tunnel in from the edge, c should be about equal to the reaction product layer thickness (~3 μm), whereupon the misfit stress should be $\sigma_0 > 600$ MPa. Such levels of misfit stress arise from the thermal expansion mismatch between either the γ-TiAl or the σ reaction layer with either the Al_2O_3 or the Ta(Ti).

V. Conclusion

In-plane stresses can have a major influence on the behavior of interface cracks. In particular, tensile in-plane stress acts in conjunction with flaws near the interface to destabilize interface cracks and causes them to depart from the interface. Conversely, compressive in-plane stresses stabilize interface cracks and essentially deactivate flaws around the interface. Such issues are important in the failure of bonds when either reaction layers or coatings subject to misfit stresses are present, and in fiber fracture from interface debonds in brittle matrix composites. The calculations are illustrated by observations of branch cracks within a reaction product layer formed in the Ti(Ta)/Al_2O_3 system.

References

[1]M.Y. He and J.W. Hutchinson, "Kinking of a Crack out of an Interface," *J. Appl. Mech.*, **56** [2] 270–78 (1989).

[2]J. R. Rice, "Elastic Fracture Mechanics Concepts for Interfacial Cracks," *J. Appl. Mech.*, **55** [1] 98–103 (1988).

[3]J.W. Hutchinson, "Mixed Mode Fracture Mechanics of Interfaces"; in *Metal/Ceramic Interfaces.* Edited by M. Rühle, A. G. Evans, M. F. Ashby, and J. P. Hirth. Pergamon Press, Elmsford, NY, 1990.

[4]T. Suga, E. Elssner, and S. Schmauder, "Composite Parameters and Mechanical Compatibility of Material Joints," *J. Comp. Mater.*, **22**, 917–34 (1988).

[5]B. Cotterell and J. R. Rice, "Slightly Curved or Kinked Cracks," *Int. J. Fract.*, **16** [2] 155–69 (1980).

[6]M.Y. He and J.W. Hutchinson, "Kinking of a Crack out of an Interface: Tabulated Solution Coefficients," Harvard University Report MECH-113A (available for a limited period from Marion Remillard, Pierce Hall 314, Division of Applied Sciences, Harvard University, Cambridge, MA 02138).

[7]A. Bartlett, M. Rühle, and A. G. Evans, "Residual Stress Cracking in Metal/Ceramic Bonds," *Acta Metall.*, in press.

[8]J. Kennedy and G. Geshwind, "Interfacial Reactions in Potential Titanium Matrix Composites"; p. 2299 in *Titanium Science and Technology.* Edited by R. I. Jaffee and H. M. Burte. Plenum Press, New York, 1973.

[9]H. E. Dève, G. R. Odette, R. Mehrabian, and A. G. Evans, "Ductile Reinforcement Toughening of γ-TiAl," *Acta Metall.*, **38**, 1491 (1990).

[10]M.Y. He and J.W. Hutchinson, "Crack Deflection at an Interface between Dissimilar Elastic Materials," *Intl. J. Solids Struct.*, **25**, 1053–67 (1989).

[11]P. G. Charalambides, J. Lund, R. M. McMeeking, and A. G. Evans, "A Test Specimen for Determining Fracture Resistance of Bimaterial Interfaces," *J. Appl. Mech.*, **56**, 77–82 (1989). □